Cognitive Methodology for Optical Amplifier Gain Adjustment in Dynamic DWDM Networks

Uiara Moura, Miquel Garrich, Heitor Carvalho, Matheus Svolenski, Alexandre Andrade, Amílcar C. Cesar, *Member, IEEE*, Juliano Oliveira, *Member, IEEE*, and Evandro Conforti, *Life Member, IEEE*

(Top-Scored)

***Abstract*—Our recently proposed cognitive methodology for optical amplifier gain adjustment, that relies on case-based reasoning, showed optical signal-to-noise ratio improvements over time demonstrating the cognition process regardless the deployed amplifier type. In this paper, we extend our preliminary analysis exploring the cognitive methodology benefits for different and larger network topologies. The obtained results show agreement between networks, demonstrating the methodology suitability regardless the network scenario.**

***Index Terms*—Case-based reasoning, cognitive networks, dynamic optical networks, optical amplifiers.**

I. Introduction

OPTICAL networks are evolving toward a reconfigurable and flexible optical layer to enable the transmission of different data rates and modulation formats [1]. Moreover, the current growth of end-users' services and applications increases traffic heterogeneity and poses additional requirements at the control and management layer.

In this context, enhanced configurations of physical-layer equipment have been proposed, such as optical amplifiers with a dynamic gain equalization [2] and a local adaptive gain control [3]–[5], both aiming at end-to-end performance improvements. Other examples are flexible transmitter and receiver architectures that adapt their modulation formats and symbol rates according to bit-error rate (BER) information [6]. Similarly, wavelength selective switches (WSSs) can be configured using global equalization strategies to improve network performance [7]. Additionally, power budget strategies that combine the control of amplifiers and WSSs jointly with routing and wavelength assignment (RWA) have proved to obtain optical signal-to-noise ratio (OSNR) improvements in meshed network scenarios [8]. All these strategies apply adaptive schemes to maintain performance and service continuity under dynamic scenarios.

The concept of cognitive networks, well known in radio technologies [9], is present in recent researches in optical networks. For instance, it is applied to reduce the connection blocking probability [10], to build a quality of transmission estimator for classifying lightpaths (LPs) [11], to dynamically adjust the modulation formats to satisfy quality of transmission requirements [12] improving failure restoration time, and to reconfigure virtual topologies [13]. Therefore, cognitive approaches and techniques applied to optical network are viable candidates to manage complexity and to permit efficient utilization of available resources in applications and services as cheap as possible [9].

In [14], we presented a cognitive methodology, which adjusts the optical amplifiers' operating points in a dynamic optical network. This methodology aims to optimize the connections' OSNR and relies on case-based reasoning (CBR) to learn from each LP establishment for OSNR improvements over time. Also in [14], a study and experimental validation for a small five-node network topology were performed, showing the learning capability and suitability for diverse amplifier types. In this paper, we extend the analysis of our global cognitive methodology to different and real network topologies, with different characteristics in terms of number of nodes and links. Current results are interesting for the operator's point of view because they show agreement between real networks scenarios, with different topologies, traffic loads, and amplifiers models, presenting OSNR improvements compared to other gain adjustments applications while remaining the learning capability.

The remainder of the paper is organized as follows. Section II presents some enhanced amplifiers control techniques, including the cognitive methodology. Section III shows some considerations about the simulation setup, regarding component models, network topologies, OSNR calculation and traffic generation. Section IV presents the experimental validation for a single path and the complete network. Section V presents the simulation results for the real network topologies and Section VI concludes this paper.

II. Enhanced Amplifier Control Techniques

Optical amplifiers, usually based on erbium-doped fiber amplifier (EDFA), are essential components in optical networks because they recover the optical signals from passive

Manuscript received October 12, 2015; revised December 2, 2015 and January 18, 2016; accepted January 25, 2016. Date of publication January 26, 2016; date of current version March 3, 2016. This work was supported by the Brazilian Ministry of Communications, FUNTTEL/FINEP, under the Project 100GETH and CNPq.

U. Moura, M. Garrich, H. Carvalho, M. Svolenski, A. Andrade, and J. Oliveira are with the CPqD Foundation—Research and Development Center in Telecommunications, Campinas, SP 13086-902, Brazil (e-mail: umoura@cpqd.com.br; miquel@cpqd.com.br; heitorc@cpqd.com.br; matheuss@cpqd.com.br; adaoud@cpqd.com.br; jrfo@cpqd.com.br).

A. C. César is with the Department of Electrical and Computer Engineering, São Carlos School of Engineering , University of São Paulo, São Carlos, SP 13566-590, Brazil (e-mail: amilcar@sc.usp.br).

E. Conforti is with the Department of Communications, Faculty of Electrical and Computer Engineering, University of Campinas, Campinas, SP 13083-970, Brazil (e-mail: conforti@ieee.org).

Color versions of one or more of the figures in this paper are available online at http://ieeexplore.ieee.org.

Digital Object Identifier 10.1109/JLT.2016.2522305

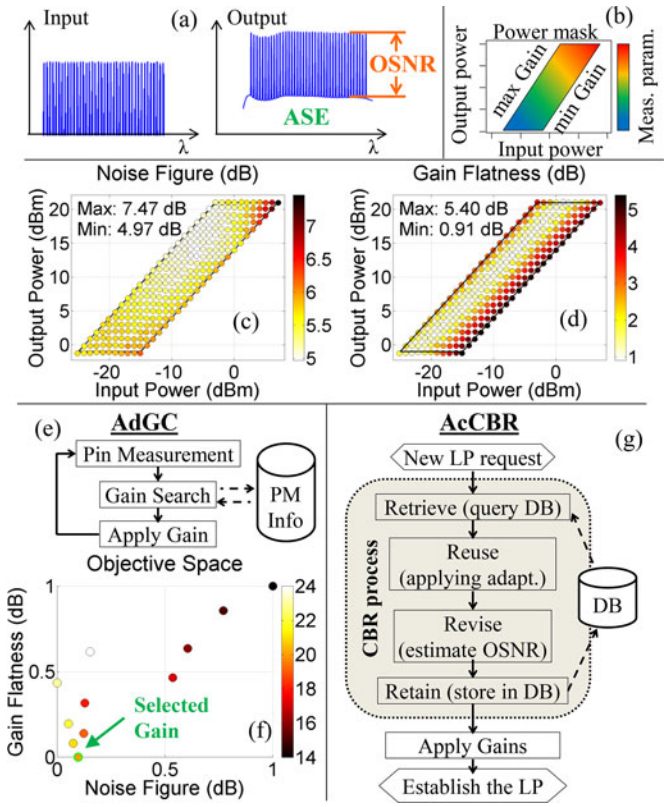

Fig. 1. (a) Input and output amplifier power spectra. (b) Power mask. Characterization results for (c) noise figure and (d) gain flatness. AdGC (e) flowchart and (f) objective space. (g) AcCBR flowchart.

components attenuations. However, amplifiers are also the main noise contributors reducing the OSNR. Moreover, since noise introduction depends on the amplifiers' operating point, it is important to find their best operating point which may lead to the lowest OSNR possible degradation.

Since an exhaustive gain-combination search for all the amplifiers would be unaffordable, especially for large and dynamic networks, some enhanced control techniques for optical amplifiers, based on local adaptive heuristics, have been proposed [3]–[5] and applied in straight line scenarios. These techniques do not guarantee a global optimal result, but as they try to find the best amplifier operating point, they end up improving end-to-end performance. On the other hand, for a dynamic and meshed optical network scenario, we proposed a global cognitive methodology in [14], which will be described in more detail in Section II-C.

These enhanced control techniques rely on an experimental amplifier characterization detailed as following.

A. Amplifier Characterization Process

The amplifier characterization process [15] consists of two steps. First, amplifier input/output total powers and spectra (see Fig. 1(a)) are experimentally and automatically measured in discrete operating points, with a pre-defined granularity, inside a region defined as the power mask [16], illustrated in Fig. 1(b). Second, the information obtained in the first step is used to calculate the performance parameters such as noise figure (NF) and gain flatness (GF). GF is defined here as the difference in dB between the highest and lowest channel gains. Fig.1(c) and (d) present the characterization results inside the power mask for worst NF among all channels and GF, respectively, for an EDFA with a maximum output power of 21 dBm, a minimum input power of –25 dBm, and a gain range from 14 to 24 dB. In this example, the characterization uses 40 dense wavelength division multiplexing (DWDM) non-modulated channels in C band (ITU-T grid) and spaced by 100 GHz. Note that the amplifier power mask provides valuable information for its control.

B. Adaptive Gain Control (AdGC)

The AdGC application, described in [3], uses the amplifier characterization outcome to adjust the amplifier operating point automatically, in terms of set point gain, to provide the best trade-off between its NF and GF. By doing so, AdGC attempts to achieve a better end-to-end performance in terms of OSNR. We restrict our analysis to amplifiers with an automatic gain control (AGC), which is a mechanism integrated to the amplifier embedded software that adjusts the amplifier pump power, using a proportional-integral controller, to provide the desired set point gain. AdGC might be applied to dynamic networks, in case of input power changes due to channel load variations or failure.

AdGC is a local application that adjusts each amplifier independently, taking into account its performance. Although optimal end-to-end performance is not guaranteed, satisfactory results for AdGC were reported in [5], in a primitive cognitive approach considering the launch power impact on BER measurements, and in [3], with some adjustments considering weights applied to NF and GF parameters, and monitoring BER values.

Fig. 1(e) depicts a high-level AdGC flowchart, in which power mask information (PM Info) is a static database and refers to the characterization outcome. The AdGC process is composed of three steps. The *Pin measurement* step monitors the amplifier total input power (Pin) and, when there is a change in its value, the *Gain search* step queries PM Info for operating points with the same current Pin. These points are plotted in an objective space, illustrated in Fig. 1(f), with NF and GF as the axis (scaled from zero to one). Each point in the objective space refers to a gain value. Finally, the *Apply Gain* step selects a gain (indicated in Fig. 1(f) with the minimum Euclidean distance from the origin), and applies it to the amplifier.

C. Amplifier Cognitive CBR (AcCBR)

A cognitive network perceives current conditions, plans, decides, acts, and learns from these adaptations to use them in future decisions, taking into account end-to-end goals [17]. AcCBR aims to optimize the connections' OSNR by applying cognition for amplifier set point gain adjustments in dynamic optical networks based on CBR. CBR is a mature autonomous machine learning technique in radio network applications now being demonstrated in academic and industrial research and is a combination of reasoning and learning [9], exploring prior experience to solve future problems [18].

Fig. 1(g) shows the AcCBR flowchart, which is a global application applied at each new LP request, before its

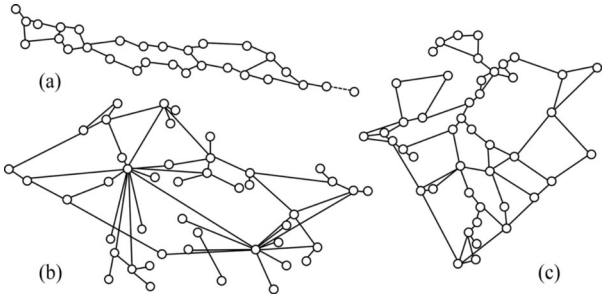

Fig. 2. (a) Biz Networks: 29 nodes, 66 links, D = 0.081. (b) CESNET: 45 nodes, 112 links, D = 0.057. (c) Palmetto: 45 nodes, 128 links, D = 0.065 [20].

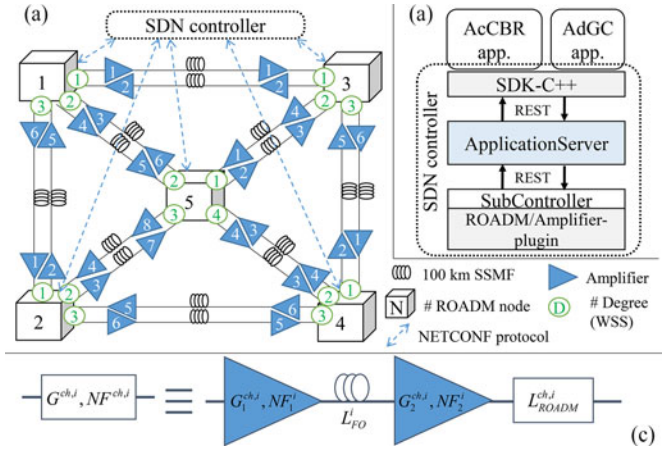

Fig. 3. (a) AN: CPqD's metropolitan optical network test-bed. (5 nodes, 16 links, D = 0.8) (b) SDN controller detail including a C++ SDK, the application server (framework for applications), and the SubController containing a ROADM-plugin. (c) Link *i* as a black box to calculate the path noise figure.

establishment. The CBR process is divided in four steps. First, the *retrieve* step queries a database (DB) for similar previous LP cases in terms of number of links, total link input power and link losses, within a margin of ±1dB. The DB is a table with the LP information of all the connections established in the network until that moment and it is built during the following CBR process steps. Second, in the *reuse* step, when there is no similar case in DB (or when DB is empty because it is the first connection), AcCBR considers the current amplifiers' gains along the LP. For a single similar case in the DB, AcCBR randomly changes by ±1 dB one amplifier gain of this similar case to explore future improvements. For two similar cases in the DB, AcCBR defines a new vector of gains $\mathbf{G}_{\text{new}}$ according to

$$\boldsymbol{G}_{\text{new}} = \boldsymbol{G}_H + \frac{\boldsymbol{G}_H - \boldsymbol{G}_L}{|\boldsymbol{G}_H - \boldsymbol{G}_L|}, \tag{1}$$

where $\mathbf{G}_{\text{H}}$ and $\mathbf{G}_{\text{L}}$ are amplifiers' gain vectors of the LP with the higher and lower OSNRs, respectively. By doing so, $\mathbf{G}_{\text{new}}$ explores the OSNR improvement direction provided by these two similar LP cases in the DB. Finally, for three or more similar cases in the DB, AcCBR applies (1), and considers one of the following alternatives:

1) Alter an amplifier gain not modified until now in the set of similar cases by ±1 dB with probability α;
2) Modify an amplifier gain that has different values in the set of similar cases with probability μ;
3) Use the outcome of (1) without any modification with probability υ.

The condition $\alpha + \mu + \upsilon = 1$ must hold. Note that these alternatives attempt to address the classical well-known exploration and exploitation trade-off in evolutionary algorithms [19]. The *revise* step estimates the OSNR at the end of the LP considering the reuse outcome ($\mathbf{G}_{\text{new}}$). As the final step in the CBR process, *retain* stores in DB the new LP information in terms of number of links, total link input powers, link losses, $\mathbf{G}_{\text{new}}$ and OSNR estimation, regardless the latter value, to serve as input for future decisions. If it is the first connection, DB is created during the retain step.

Finally, AcCBR adjusts the amplifiers' gains along the LP according to the best case in DB in terms of OSNR (which might not be the one just stored) and establishes the new LP.

AcCBR is restrict to transparent optical networks and should be applied together with the RWA, since changes in the amplifiers total input power will enrich the diversity of the DB content. We recall that, differently from the AdGC's static DB (PM Info), the AcCBR's DB increases over time.

Our proposed methodology was first presented in [14] as EDFA cognitive CBR. However, this application is not restrict to one amplifier technology, and may be applied to any amplifier, such as Raman or hybrid amplifiers, since it has been characterized in terms of NF and GF under its power mask and has an AGC as described in Section II-B.

III. Simulation Setup

A. Components' Models

As described in the previous section, the *revise* step performs an estimation (and not a measure) of the LP quality, because $\mathbf{G}_{\text{new}}$ cannot be applied until the end of the AcCBR process, in which it selects the best case in DB that may not correspond to $\mathbf{G}_{\text{new}}$. Thus, this OSNR estimation must assume models for the network components such as optical fibers, optical amplifiers and reconfigurable optical add-drop multiplexers (ROADMs).

The amplifier model used in this paper is restricted to the following assumptions, based on the characterization outcome: NF dependence on operating point, but not on the channel frequency; and gain dependence on channel, in order to simulate the accumulated tilt effect along a cascade of amplifiers. The NF assumption may cause discrepancies between simulation and experimental OSNRs due to NF variations higher than 1 dB across the C band. However, it can be negligible in this first approach since we aim to evaluate if the AcCBR methodology will properly work. Moreover, experimental OSNR measurements presented in Section IV-D (see Fig. 5(c)–(e)) show agreement with the OSNR estimation (simulation) even not considering NF dependence on channel.

The optical fiber model assumes fixed attenuation independent to channel. Considerations of non-linear effects are outside the scope of this paper. However, we consider that the most powerful channel at the input of all optical fibers has up to 0 dBm to avoid nonlinearities.

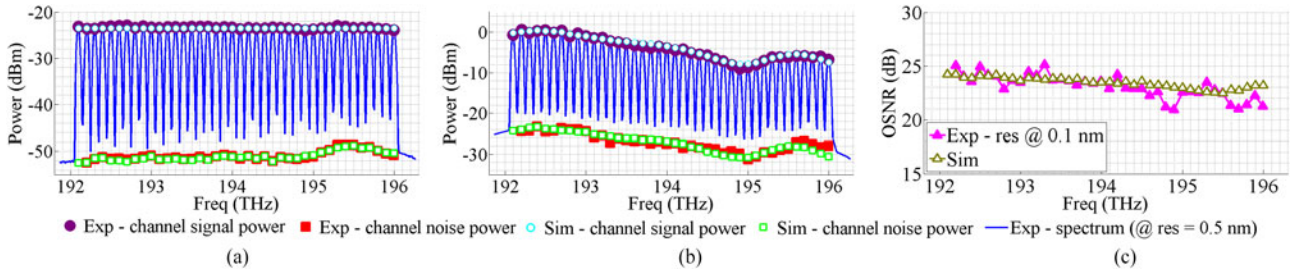

Fig. 4. Single path results in terms of (a) Input power signal and noise, with spectrum, (b) output power signal and noise, with spectrum and (c) OSNR.

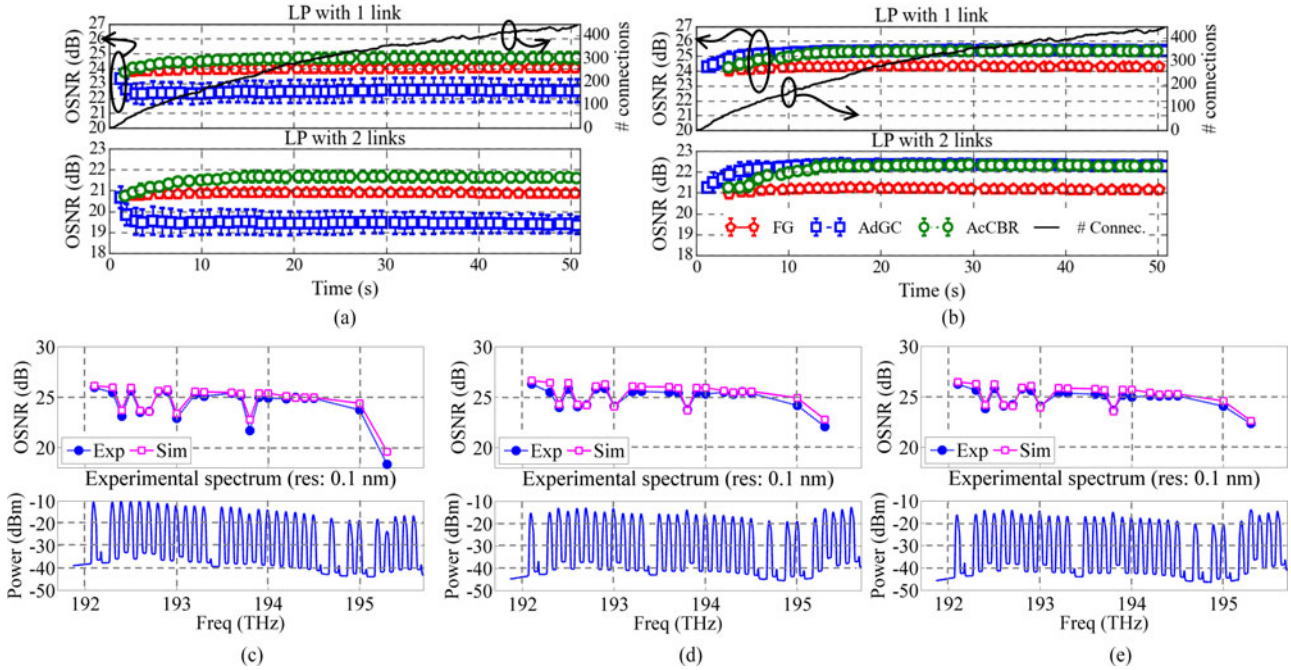

Fig. 5. AN simulation results in terms of OSNR and total number of connections for (a) *B21/P14* and (b) *B21/B21*. Experimental measurements at AN node 1 and drop port degree 1 for (c) FG, (d) AdGC and (e) AcCBR.

The ROADM model considers an attenuation per channel, dynamically adjusted to equalize the channels power level at the first amplifier input on the next link.

B. Network Topologies

We analyze four different network topologies in this paper. The first one, CPqD's metropolitan optical meshed network, illustrated in Fig. 3(a), referred as autonomous network (AN), is used to validate the simulation tool in terms of component models and OSNR estimation. Section IV-A physically details the AN.

To validate the versatility of our methodology against different network topologies in simulation, we choose three real networks from [20], shown in Fig. 2. For these networks, we assume bidirectional links (directed graphs). The density of a directed graph G(V,E), where V is the set of vertices (nodes) and E is the set of edges (links), is defined as the current number of edges divided by the total possible number of edges: $D = |E|/(|V|(|V| - 1))$ [21]. Density indicates the graph connectivity, measuring how close a graph is to its corresponding complete graph. We restrict our work to small networks (instead of typical country dimensional) with link distances near 100 km, which is the distance considered for the networks in this paper to support two amplifiers per link.

Biz Networks (see Fig. 2(a)) is an Indonesian network and is the smallest network in terms of number of nodes, but with the highest density (only behind AN, with D = 0.8). It contains five rings interconnected, leading to LPs with high number of links. CESNET (see Fig. 2(b)) is from Czech Republic and has the particularity to have few nodes with a high connectivity degree and a considerable number of nodes (more than 50%) with just one connection. Because of this characteristic, it has the lowest graph density and LPs with the smallest number of links. Finally, Palmetto (see Fig. 2(c)) is from South and North Caroline, USA, and is numerically similar to CESNET (in terms of number of nodes, links and density), but with a very different topology.

C. OSNR Calculation

For the signal point of view, each link in Fig. 3(a) is a black box with an equivalent NF and gain, as illustrated in Fig. 3(c). The equivalent noise figure for link i and channel CH can be

calculated considering an association of amplifiers and loss components in cascade, which leads to [22]:

$$NF^{\mathrm{CH},i} = NF_1^i + \frac{NF_2^i}{G_1^{\mathrm{CH},i} L_{\mathrm{FO}}^i}, \tag{2}$$

Where NF_1^i and NF_2^i are noise figures for the first and the second amplifier, respectively, $G_1^{\mathrm{CH},i}$ is the channel gain for the first amplifier, and L_{FO}^i is the fiber loss. All these parameters are linear and NF and gain are obtained in the characterization process, according to the components' models described in Section III-A.

Link *i* gain is calculated according to

$$G^{\mathrm{CH},i} = G_1^{\mathrm{CH},i} L_{\mathrm{FO}}^i G_2^{\mathrm{CH},i} L_{\mathrm{ROADM}}^{\mathrm{CH},i}, \tag{3}$$

where $G_2^{\mathrm{CH},i}$ is the channel gain for the second amplifier and $L_{\mathrm{ROADM}}^{\mathrm{CH},i}$ is the ROADM loss.

The ROADM loss is not considered to calculate the link NF in (2) because it is at the end of the link, not contributing to noise addition or reducing the power level at amplifier's input. However, it will be considered on the path equivalent NF, as we shall see, since it reduces the input power in the first amplifier on the next link.

As a path is composed of a cascade of links, we can estimate its NF by [22]:

$$NF^{\mathrm{CH,path}} = NF^{\mathrm{CH},1} + \frac{NF^{\mathrm{CH},2}}{G^{\mathrm{CH},1}} + \ldots + \frac{NF^{\mathrm{CH},n}}{G^{\mathrm{CH},1} \ldots G^{\mathrm{CH},n-1}}, \tag{4}$$

for a LP with *n* links and with $NF^{\mathrm{CH},i}$ and $G^{\mathrm{CH},i}$ as in (2) and (3), respectively, for the *i-th* link.

The total path gain for channel *CH* is

$$G^{\mathrm{CH,path}} = G^{\mathrm{CH},1} \ldots G^{\mathrm{CH},n}. \tag{5}$$

Finally, channel OSNR at the end of the path can be estimated using [22]

$$NF^{\mathrm{CH}} = \frac{P_{\mathrm{ASE}}^{\mathrm{CH}}}{h\nu^{\mathrm{CH}} \Delta\nu^{\mathrm{CH}} G^{\mathrm{CH}}} + \frac{1}{G^{\mathrm{CH}}}, \tag{6}$$

where $P_{\mathrm{ASE}}^{\mathrm{CH}}$ is the channel noise power (in W), or the amplified spontaneous emission (ASE) power due to the amplifier under characterization (illustrated in the output spectrum in Fig. 1(a)); *h* is the Planck's constant (in $\mathrm{m^2kg/s}$); ν is the channel frequency; $\Delta\nu^{CH}$ is the channel band in which signal and noise were measured (both in Hz) and G^{CH} is the channel gain.

Substituting NF^{CH} by (4), G^{CH} by (5) and $P_{\mathrm{ASE}}{}^{\mathrm{CH}}$ by $OSNR^{\mathrm{CH}} G^{\mathrm{CH,path}} P_{\mathrm{in,link}}^{\mathrm{CH}}$ in (6) yields

$$OSNR^{\mathrm{CH}} = \frac{G^{\mathrm{CH,path}} P_{\mathrm{in,link}}^{\mathrm{CH}}}{\left(G^{\mathrm{CH,path}} NF^{\mathrm{CH,path}} - 1\right) h\nu^{\mathrm{CH}} \Delta v^{\mathrm{CH}}}, \tag{7}$$

where $G^{\mathrm{CH,path}}$ and $NF^{\mathrm{CH,path}}$ are linear, $P_{\mathrm{in,link}}^{\mathrm{CH}}$ is the channel power input in the first link (in W). As (7) is adapted from (6), the input signal must be free of noise.

In the general case, the link distance defines the number of amplifiers and the length/number of fiber spans between two nodes. In such cases, we can still use OSNR estimation in (7), after updating the equations (2) and (3) considering the current components in the link. However, in this paper, we restrict our study to links with one fiber span and two amplifiers.

D. Traffic Generation and RWA Assumptions

The computer simulation, developed in MATLAB, considers a classical optical circuit-switched network, with *ad hoc* dynamic demand and traffic generated according to a Poisson process, with connections arrival time and duration modeled by a negative exponential distribution. We work with 1000 connections and low/high traffic loads. The values of each one is according to its block probability and depends on the network topology. A low load leads 0% of block probability and high load is for the maximum block probability.

AdGC and AcCBR are methodologies designed to be applied together with the RWA, so that every time a new LP is established, causing changes in the amplifiers total input power, it is necessary to adjust their operating point based on a local/global performance (AdGC/AcCBR, respectively).

We assume a transparent optical network, with wavelength continuity constraint, since the LP must have the same wavelength available in all links. To establish the connection, there are available 40 channels at C band, 100 GHz spaced and there is no grooming. Thus, every new connection uses a new channel, even if some existing channel has available band to support this new connection. We apply Djikstra to find the path with the lowest loss, and consider *first-fit* to wavelength assignment in unidirectional connections (Simplex).

IV. Experimental Validation

We perform some experiments at the AN test bed available in our laboratory in order to validate the components' models and the OSNR estimation by (7) presented in Sections III-A and C, respectively. Thus, we can guarantee that the simulation results are reliable, especially for networks not physically available to perform experiments.

A. Experimental Network Test-Bed

Experimental validation considers the AN test-bed depicted in Fig. 3(a). AN consists of four ROADMs of degree 3 and a central ROADM of degree 4, leading to a network with a high density. All ROADMs in the network have a broadcast-and-select (BS) structure. Two EDFAs (single stage) with a maximum output power of 21 dBm for each standard single mode fiber (SSMF) 100-km span compensate fiber (0.2 dB/km) and ROADM losses. The transmitter has 40 continuous-wave lasers (ITU-T DWDM grid from C21 to C60), 100 GHz spaced, modulated by four multiplexed lines of 32 Gb/s (PRBS $2^{31}-1$) that generate 128 Gb/s DP-QPSK channels. Channels occupy 50 GHz alternate slots in the spectrum enabling proper OSNR measurements considering the adjacent noise. However, as AcCBR already estimates the OSNR, these measurements are performed just to compare simulation and experimental results, allowing operators to use full loaded 80 channels. A 1×16 splitter is used after the transmitter setup in order to feed the 16 add ports of the network. The input power per channel at the first amplifier of each link is set

to −25 dBm using the WSSs attenuation capability. The drop ports are connected to a 16 × 1 optical switch for automatic optical spectrum analysis. Thus, it is possible to establish a connection between any two nodes in the network. Recovering the transmitted information using off-line digital signal processing algorithms is outside the scope of this paper.

B. Software Defined Networking (SDN) Control

An SDN controller communicates to the network components and runs the amplifier advanced gain control applications. Fig. 3(b) shows CPqD's three-layer-based SDN controller which runs AcCBR and AdGC as high-level network applications. It includes a C++ software development kit (SDK); an application server, which performs the role of control layer that manages the network controllers and provides a framework for network applications (e.g., alarm handling, statistics calculation and application authentication) and a SubController, containing a ROADM/Amplifier-plugin as a driver to abstract the communication protocol with the network equipment.

C. Single Path Validation

To validate the estimated channel OSNR using (7) and the components' models, a path with two links in AN, from node 1 to node 4, passing through node 3 (see in Fig. 3(a)) was full loaded (40 channels) and all channels OSNR were measured and estimated in node 4 experimentally and in simulation, respectively, with no algorithm applied. Fig. 4 shows the results in which EDFAXY means EDFA Y from node X. Fig. 4(a) compares experimental and simulation results at the path input (input of EDFA 1 in node 1). It presents the spectrum measurements with a resolution of 0.5 nm, used to measure the experimental signal power. Experimental noise power is estimated from the OSA measurements for OSNR, at a resolution of 0.1 nm. It is possible to see a great match between simulation and experimental for signal and noise powers for all 40 channels.

Fig. 4(b) presents the same parameters at the path output (output of EDFA 1 in node 4). Signal powers also match for all channels, while noise powers present small differences between experimental and simulation values of up to 2 dB around the region of high frequency.

These differences also appear in Fig. 4(c), which compares the experimental measurements for OSNR (performed by the OSA at a resolution of 0.1 nm) and the simulated OSNR, estimated using (7). In any case, despite these small discrepancies around 2 dB, we observed an agreement between simulation and experimental OSNRs because they follow a similar trend. Note that noise estimation considering the same amplifier NF for all channels, described in Section III-A, and WSS filtering may cause these differences.

D. Network Validation

AN was completely validated considering three different amplifier control conditions: fixed gains (FG), AdGC and AcCBR. In FG, amplifiers' gains are set to compensate fiber and ROADM losses and never change. AdGC and AcCBR act as presented in Section II. For AcCBR, at the simulation beginning, the network is set as in FG. Thus, as when there is no similar case in DB AcCBR considers the current gains, FG can be seen as the initial condition for AcCBR. Before the experiment, we performed some simulations with the same traffic (1000 connections and 500 erlang), solving a traditional RWA problem. In addition, we consider two different cases of amplifier models for each link detailed in Fig. 3(c). The first case is the *B21/P14*, which considers a booster amplifier with up to 21 dBm of total output power (B21) placed just before the optical fiber and a preamplifier with up to 14 dBm of total output power (P14), placed after the optical fiber. The second case is the *B21/B21*, which considers that all amplifiers in the network (before and after the optical fibers) are booster amplifiers (B21). All these amplifiers are EDFA with a single stage. For AcCBR methodology, the DB starts empty and increases along the time.

TABLE I
EXPERIMENTAL RESULTS FOR NETWORK VALIDATION

LP size	1 link	2 links
OSNR (dB)	Mean ± std δ	Mean ± std δ
FG	24.09 ± 1.49	18.57 ± 3.44
AdGC	24.78 ± 1.30	22.37 ± 1.88
AcCBR	24.76 ± 1.02	22.59 ± 1.29

Fig. 5 shows the network validation, comparing simulation and experimental results. Fig. 5(a), (b) show the simulation OSNR (mean and standard deviation) results for all the connections presented at the network in a time interval as a function of the connection start time. Fig. 5(a) stands for *B21/P14* case, while Fig. 5(b) stands for *B21/B21*. Besides, since all connections in AN have up to two links, upper graphs in Fig. 5(a) and (b) are for LP with one link and bottom graphs for LP with two links. Upper graphs on Fig.5(a) and (b) also show the number of total connections present at the network, which is the same for both cases of amplifier models since they consider the same traffic.

For B21/P14, FG remains almost constant along all simulation, with values around 24 and 21 dB for 1 and 2 link/LP, respectively. AdGC presents the worst results, with the OSNR decreasing from around 23.5 to 22.5 dB, and from 21 to around 19 dB for 1 and 2 link/LP, respectively, at the beginning of the simulation, and remaining near this later value. AcCBR, on the other hand, presents the best results, with an increase of OSNR values at the beginning of the simulation, due to the learning process, and achieving almost 24.5 and 22 dB for LPs with 1 and 2 links, respectively.

For B21/B21 models, FG and AcCBR present the same behavior as in B21/P14 case, while AdGC has the opposite behavior, increasing the OSNR at the beginning of the simulation from 24 to 25.5 dB and from 21 to values higher than 22 dB, for 1 and 2 link/LP, respectively, reaching the same results as AcCBR. These different OSNR behaviors of AdGC for these two cases show its performance dependence on the amplifiers models used in the network. On the other hand, it is important to point out that AcCBR reaches the best performance in both cases, showing its robustness to the amplifiers models.

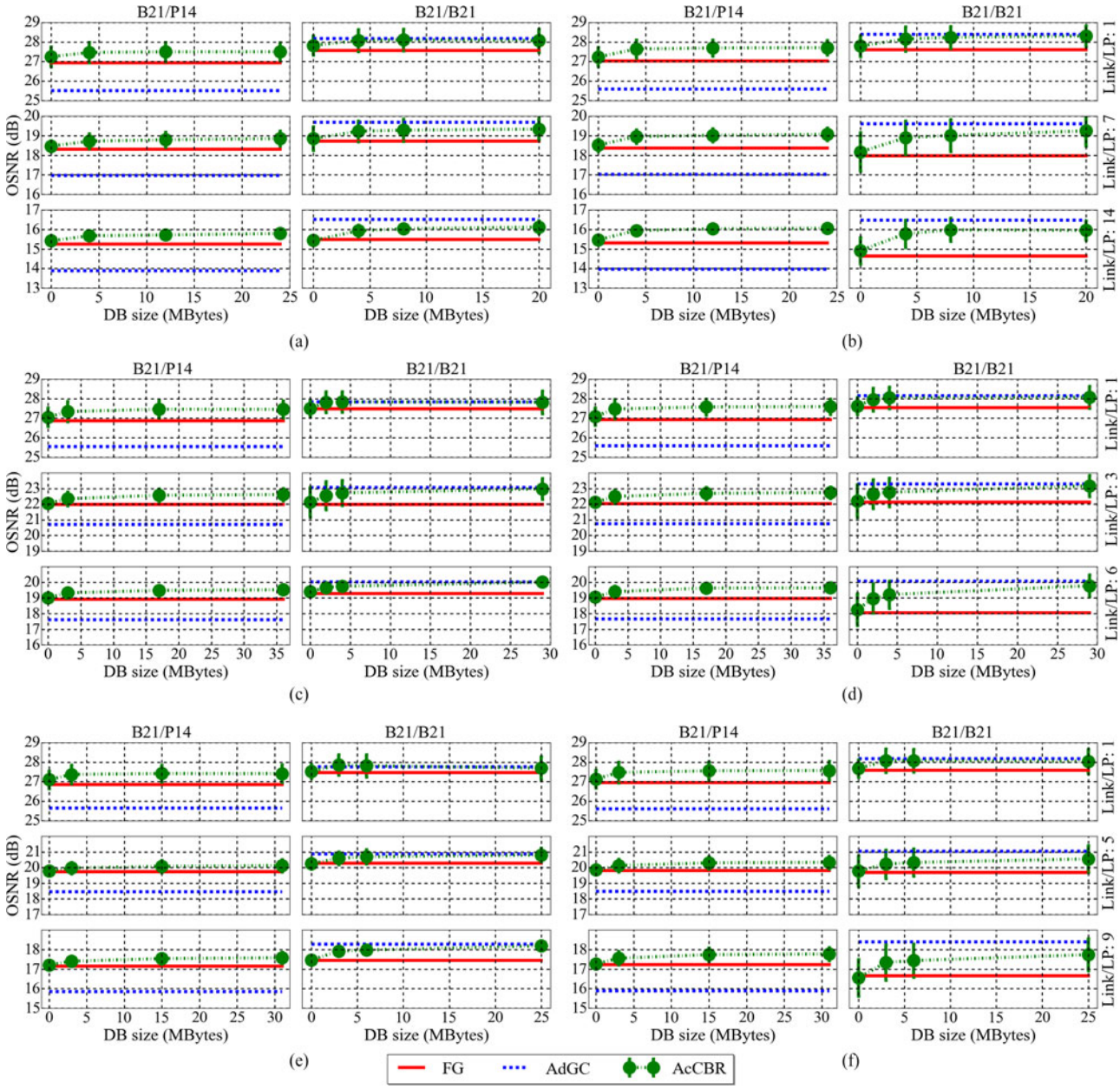

Fig. 6. Mean OSNR at the end of the LP per DB size. Biz Networks, (a) load = 100 erlang, (b) load = 800 erlang; CESNET, (c) load = 200 erlang, (d) load = 1600 erlang; Palmetto, (e) load = 100 erlang, (f) load = 900 erlang.

To validate the simulation results we perform an experiment that consists of taking a snapshot near 50 s in Fig. 5(b) considering all the connections presented in the network and the amplifier gains for the three amplifier controls (FG, AdGC and AcCBR). Then, we measure the OSNRs experimentally for all 16-drop ports and compare with the simulation results.

Fig. 5(c), (d) and (e) show the comparison between simulated and experimental OSNR results for FG, AdGC and AcCBR, respectively, for all channels dropped at node 1 and port drop degree 1. It is possible to identify the channels with one (high OSNR) and two (low OSNR) links/LP and the best performance for AdGC and AcCBR compared to FG. These OSNR comparisons validate the simulation tool in terms of component models and OSNR estimation for all network nodes. The experimental spectra associated to the OSNR (upper graph) is shown at the bottom of Fig. 5(c)–(e). Note that the splitter stage in the passive BS ROADM structure provides multiple copies of the input signals for selective filtering at the WSS stage, thus bypassing channels appear at the drop port (spectra plots) but not in the OSNR plots (dropped channels).

Table I presents the experimental results in terms of mean and standard deviation OSNR measurements at all drop ports for each methodology at the same snapshot time considered in Fig. 5(c)–(e). In Table I, FG also presents the worst result, with a degradation of up to 4 dB in mean OSNR, while AdGC and AcCBR performances are very close to each other, just as in Fig. 5(b). The differences in mean OSNR for FG and LP with two links between Fig. 5(b) and Table I are within experimental standard deviation margim. It is worth mentioning that, although AcCBR considers just the new connections OSNRs, it is

possible to extend the performance to other connections already presented on the network, since there is an improvement on the mean OSNR of all connections.

V. Results and Discussions

For the networks described in Section III-B (except AN) we perform simulations (also developed in MATLAB) to solve a traditional RWA for a traffic with 1000 connections assuming that each link has a 100 km of SSMF and two optical amplifiers. These simulations were repeated ten times for each network, for each amplifier gain control conditions (FG, AdGC and AcCBR), for each amplifier models per link (*B21/P14* and *B21/B21*), and for each load condition (low and high, as defined in Section III-D). Moreover, we consider four cases with different initials DB sizes for AcCBR, starting from zero and sequentially increasing.

Biz Networks shows LPs with up to 17 links, due to its characteristics of ring connections, while CESNET has up to 10 links/LP, due to its hub characteristics, and Palmetto have up to 15 links/LP.

Fig. 6 summarizes the results, showing mean OSNR values for all the connections presented in the network. For the subfigures in Fig. 6, upper, middle and bottom graphs stand to LPs with 1/1/1, 7/3/5 and 14/6/9 links for Biz/CESNET/Palmetto, respectively. Left and right graphs are for *B21/P14* and *B21/B21* cases, respectively. AcCBR OSNR's (mean and standard deviation for the ten repetitions) are plotted as a function of DB size, while FG and AdGC OSNR's (just mean) are continuous to serve as a reference for AcCBR results. From these simulation results, it is possible to observe the same behavior previous seen in AN results (see Fig. 5(a), (b)), i.e., AdGC and FG presenting the worst performance for *B21/P14* and *B21/B21* cases, respectively.

It is important to recall that AN single simulation for one traffic pattern with 1000 connections reported in Section IV-D was sufficient for AcCBR reach a good performance at the end of the simulation (see Fig. 5(a), (b)). This occurs because, for a small network such as AN, the set of possible cases is also small, and a DB size with a magnitude of kiloBytes has sufficient cases to help AcCBR obtain good solutions. However, this is not true for bigger networks such as Biz, CESNET and Palmetto.

Backing to Fig. 6, for AcCBR with an empty DB, the performance is near FG, which is expected, since FG is the initial condition for AcCBR (when there is no similar case in DB). For bigger networks, the set of possible cases is also bigger (because the diversity of LP's in terms of link number) in a way that we need a magnitude of megabytes to have a DB with sufficient cases to improve AcCBR results.

Note that, similar to the simulation results for AN (see Fig. 5(a), (b)), there are different OSNR performances when we apply AdGC: *B21/P14* presents the worst performance and *B21/B21* presents the best one. On the other hand, AcCBR improves the OSNR as the DB increases, showing its learning capability for *B21/P14* and *B21/B21*. Moreover, for high DB sizes, AcCBR achieves the best OSNR results for all cases, considering the standard deviation, showing its robustness regardless the amplifier models used in the network.

Moreover, the traffic load increase has an effect on the mean OSNR for *B21/B21* and FG condition: OSNR degrades as the load increase. This degradation, of up to 1.2 dB, is more perceptible for LP with high number of links. It occurs because, for FG condition, load increase leads to a higher input power at the amplifiers and, depending on the amplifier gain (see Fig. 1(c)); a degradation in NF (OSNR) can occur particularly if the amplifier is operating with a low gain.

On the other hand, AdGC presents small variations of OSNR (up to 0.2 dB) with traffic load because when the input power change, AdGC searches a new operating point with a better NF. For AcCBR, even starting with a low OSNR for empty DB, for high loads OSNR achieves almost the same results as for low load case in high DB size (with differences of up to 0.2 dB), showing AcCBR suitability in terms of initial conditions and traffic load.

Thus, regardless the network topology/size, amplifier models, traffic load and LP size (in terms of number of links), it is possible to see the learning processing happening for AcCBR methodology with OSNR improvements of up to 2 dB as DB size increase, achieving the best performance in terms of OSNR results, after the learning process.

VI. Conclusion

We proposed and validated a CBR-based cognitive methodology for optical amplifier gain adjustment for dynamic optical networks. Reported results confirmed the learning capability of the proposed methodology and its suitability regarding network topology, size and amplifier models. Future works include different exploration alternatives, and experiments considering BER measurements to explore nonlinearities for the proposed AcCBR.

References

[1] J. P. Fernandez-Palacios, V. Lopez, B. Cruz, and O. Gonzalez de Dios, "Elastic optical networking: An operators perspective," in *Proc. Eur. Conf. Opt. Commun.*, Cannes, France, pp. 1–3.

[2] V. V. Nascimento, J. C. R. F. de Oliveira, V. B. Ribeiro, and A. C. Bordonalli, "Dynamic gain equalization for erbium doped fiber amplifiers based on optoceramic sinusoidal filter cascade," *Microw. Opt. Technol. Lett.*, vol. 53, no. 3, pp. 623–626, Mar. 2011.

[3] U. C. de Moura, J. R. F. Oliveira, J. C. R. F. Oliveira, and A. C. Cesar, "EDFA adaptive gain control effect analysis over an amplifier cascade in a DWDM optical system," in *Proc. SBMO/IEEE MTT-S Int. Microw. Optoelectron. Conf.*, Rio de Janeiro, Brazil, 2013, pp. 1–5.

[4] E.de A. Barboza, C. J. A. Bastos-Filho, J. F. Martins-Filho, U. C. de Moura, and J. R. F. de Oliveira, "Self-adaptive erbium-doped fiber amplifiers using machine learning," in *Proc. SBMO/IEEE MTT-S Int. Microw. Optoelectron. Conf.*, Rio de Janeiro, Brazil, 2013, pp. 1–5.

[5] J. Oliveira *et al.*, "Demonstration of EDFA cognitive gain control via GMPLS for mixed modulation formats in heterogeneous optical networks," in *Proc. Optical Fiber Commun. Conf.*, Anaheim, CA, USA, 2013, pp. 1–3.

[6] H. Y. Choi, L. Liu, T. Tsuritani, and I. Morita, "Demonstration of BER-adaptive WSON employing flexible transmitter/receiver with an extended Open Flow-based control plane," *IEEE Photon. Technol. Lett.*, vol. 25, no. 2, pp. 119–121, 2013.

[7] E. Magalhães *et al.*, "Global WSS-based equalization strategies for SDN metropolitan mesh optical networks," in *Proc. Eur. Conf. Opt. Commun.*, Cannes, France, 2014, pp. 1–3.

[8] X. Wang, Y. Fei, M. Razo, A. Fumagalli, and M. Garrich, "Network-wide signal power control strategies in WDM networks," in *Proc. Int. Conf. Opt. Netw. Des. Model.*, Pisa, Italy, May 2015, pp. 218–221.

[9] H. M. Qusay Ed., *Cognitive Networks: Towards Self-aware Networks*. Chichester, England: Wiley, 2007.
[10] I. Rodríguez *et al.*, "Minimization of the impact of the TED inaccuracy problem in PCE-based networks by means of cognition," in *Proc. Eur. Conf. Opt. Commun.*, London, U.K., 2013, pp. 1–3.
[11] T. Jiménez, J. C. Aguado, I. de Miguel, R. J. Duran, M. Angelou, N. Merayo, P. Fernandez, R. M. Lorenzo, I. Tomkos, E. J. Abril, "A cognitive quality of transmission estimator for core optical networks," *J. Lightw. Technol.*, vol. 31, no. 6, pp. 942–951, 2013.
[12] R. Borkowski *et al.*, "Advanced modulation formats in cognitive optical networks: EU project CHRON demonstration," presented at the Optical Fiber Communication Conf., San Francisco, CA, USA, 2014, pp. 1–3, Paper W3H.1.
[13] R. Borkowski, R. Duran, C. Kachris, D. Siracusa, A. Caballero, N. Fernandez, D. Klonidis, A. Francescon, T. Jimenez, J. Aguado, I. Miguel, E. Salvadori, I. Tomkos, R. Lorenzo, I. Monroy, "Cognitive optical network testbed: EU project CHRON," *IEEE J. Opt. Commun. Netw.*, vol. 7, no. 2, pp. A344–A355, Feb. 2015.
[14] U. Moura *et al.*, "SDN-enabled EDFA gain adjustment cognitive methodology for dynamic optical networks," in *Proc. Eur. Conf. Opt. Commun.*, Valencia, Spain, 2015, pp. 1–3.
[15] C. J. A. Bastos-Filho *et al.*, "Mapping EDFA noise figure and gain flatness over the power mask using neural networks," *J. Microw. Optoelectron. Electromagn. Appl*, vol. 12, no. SI-2, pp. 128–139, Jul. 2013.
[16] WRA-219 Multichannel Erbium-Doped Fiber Amplifier, Lumentum. (2015). [Online]. Available: www.lumentum.com.
[17] R.W. Thomas, D. H. Friend, L. A. da Silva, and A. B. Mackenzie, "Cognitive networks: Adaptation and learning to achieve end-to-end performance objectives," *IEEE Commun. Mag.*, vol. 44, no. 12, pp. 51–57, Dec. 2006.
[18] R. Mantaras, "Retrieval, reuse, revision and retention in case-based reasoning," *Knowl. Eng. Rev.*, vol. 20, no. 3, pp. 215–240, 2005.
[19] M. Črepinšek, S.-H. Liu, and M. Mernik, "Exploration and exploitation in evolutionary algorithms: A survey," *ACM Comput. Surveys*, vol. 45, no. 3, pp. 35.1–35.33, Jun. 2013.
[20] The Internet Topology Zoo. (2015). [Online]. Available: www.topology-zoo.org/
[21] B. Hoppe.(2009). Webwhompers.[Online]. Available: http://webwhompers.com/graph-theory.html
[22] P. C. Becker, N. A. Olsson, and J. R. Simpson, *Erbium-Doped Fiber Amplifiers: Fundamentals and Technology*. San Diego, CA, USA: Academic, 1999.

Uiara Moura was born in Cabo de Santo Agostinho, Pernambuco, in 1983. She received the B.S. and M.S degrees in electrical engineering from the University of São Paulo, São Carlos, Brazil, in 2011 and 2014, respectively. She is currently working toward the Ph.D. degree in electrical engineering at the State University of Campinas, Campinas, Brazil. She holds four patents, and is the coauthor of 16 papers in Brazilian and international journals and conferences. She has been a Telecommunications Researcher at CPqD Foundation, Campinas, Brazil, since 2011, where she is currently involved in the high-performance optical amplifier design and in advanced amplifiers control.

Miquel Garrich was born in Barcelona, Spain, on June 29, 1982. He received the telecommunications engineering degree from Universitat Politecnica de Catalunya, Barcelona, Spain, in October 2009, and the Ph.D. degree from Politecnico di Torino, Torino, Italy, in February 2013. From July 2011 to April 2012, he was a Visiting Researcher with the School of Computer Science and Electronic Engineering (High-Performance Networks Group), University of Essex, Colchester, U.K. He is currently a Senior Researcher at the Optical Systems Division at CPqD Foundation, Campinas, Brazil. He coordinates several activities in CPqD's optical networks team, including amplifiers, ROADMs, SDN, and NFV. He has coauthored more than 20 technical–scientific papers.

Heitor Carvalho received the electrical engineering degree from Universidade de São Paulo, São Carlos, Brazil, in December 2012, and is currently working toward the Master's degree at Universidade de Campinas, Campinas, Brazil. He is currently a Junior Researcher in the Optical Systems Division at CPqD Foundation, Campinas. He executes several activities in CPqD's optical networks team, including firmware development for amplifiers, WSS and other optical-related equipments, network control software, and SDN-based applications.

Matheus Svolenski was born in Curitiba, Brazil, in 1992. He is currently working toward the B.Sc. degree in computer science from the State University of Campinas, Campinas, Brazil. He studied a year at Georgia Institute of Technology, Atlanta, GO, USA. He is currently a Telecommunications Researcher Intern in the Optical Technologies Division at CPqD Foundation, Campinas, where he works with reconfigurable optical add/drop multiplexersand optical networks including software-defined networks.

Alexandre Andrade was born in Campinas, São Paulo, Brazil, in 1993. He is currently working toward the B.S. degree in electrical engineering at Universidade Estadual de Campinas, Campinas, Brazil. He is currently in an internship program in the Optical Systems Division at CPqD Foundation, Campinas. He is working on optical mesh networks and fiber-optic communication systems. His research interests include telecommunications systems, high-performance optical mesh networks, software-defined networking, and optical technology.

Amílcar C. César received the B.S. degree in electrical engineering from the University of São Paulo, São Carlos, Brazil, in 1976, and the M.S. and Ph.D. degrees in electrical engineering from the State University of Campinas, Campinas, Brazil, in 1982 and 1990, respectively. Since 1977, he has been with the Department of Electrical and Computer Engineering, School of Engineering of São Carlos, University of São Paulo, where he is currently a Full Professor. His research interests include optical communications and microwave devices, with emphasis on numerical methods applied to the modeling of propagation of electromagnetic waves in dielectric and nonreciprocal guides, and algorithms for solving resource allocation problems in optical and wireless networks.

Juliano Rodrigues Fernandes de Oliveira (M'14) was born in Nilópolis, Brazil, in 1982. He received the degree in electrical engineering from the Federal University of Campina Grande, Campina Grande, Brazil, in2005, and the M.Sc. degree in electrical engineering from Campinas State University, Campinas, Brazil, in 2008, and is currently working toward the Ph.D. degree at São Paulo University, São Carlos, Brazil. He participated in eight research and development projects in optical communications at CPqD Foundation, leading two projects, producing three patents, and 20 publications between journals and conferences. Today, he is leading research and development projects at optical communications sub-systems at CPqD Foundation, with emphasis in Optical amplifiers (EDFA and Raman), ROADMs, and reconfigurable/autonomous optical networks.

Evandro Conforti (S'81–M'83–SM'92–LM'15) was born in S. J. Rio Preto, SP, Brazil, on August 30, 1947. He received the B.Sc. degree in electronic engineering from the Technological Institute of Aeronautics, São José dos Campos, Brazil, in 1970, the M.Eng. degree from the Federal University of Paraiba, João Pessoa, Brazil, in 1972, the M.A.Sc. degree from the University of Toronto, ON, Canada, in 1978, and the Ph.D. degree in electrical engineering from the State University of Campinas, Campinas, Brazil, in 1983. He has been with the University of Campinas (Unicamp) since 1981, where he was the Dean of the Faculty of Electrical and Computer Engineering in 1984–1987, and is currently an invited Professor of electrical engineering at FEEC. He was a Visitor at the University of Illinois at Urbana-Champaign in 1992–1994, working with the research team of Prof. S.-M. (Steve) Kang. He received the Academic Merit Medal Prof. A. J. Giarola from the Brazillian Society of Microwaves and Optoelectronic in 2014, Unicamp Inventors Prizein 2013,1º Werner von Siemens Technologic Innovation Prize (3º place Cat. Researcher) from Siemens Brazil in 2005,the ZeferinoVaz Academic Achievements Prize from Unicamp in 2005,the 1998 Brazilian Invention Prize, and the 1983 Unicamp Research Prize. He holds 14 patents and is the coauthor of a book and more than 170 papers in brazilian and international journals and conferences. He has graduated 11 Ph.D. students and 28 M.Sc. students. His current research interests include semiconductor optical amplifiers, optical coherent communication, all optical switching, and electromagnetic measurements.